

## ADSORPTION PROPERTIES OF ACIDIC AND BASIC PROTEINS ON THE SURFACE OF CARBONATE-CONTAINING HYDROXYAPATITE

Toru Kanno<sup>1\*</sup>, Toru Sendai<sup>2</sup>, Kiyoshi Tada<sup>2</sup>, Jun-ichi Horiuchi<sup>2</sup>, Toshiyuki Akazawa<sup>3</sup>,  
(\*Corresponding author: kannotr@mail.kitami-it.ac.jp)

<sup>1</sup>International Center, Kitami Institute of Technology, 165 Koen-cho, Kitami 090-8507 Japan.

<sup>2</sup>Department of Applied and Environmental Chemistry, Kitami Institute of Technology, 165 Koen-cho, Kitami 090-8507 Japan.

<sup>3</sup>Hokkaido Industrial Research Institute, Nishi-11, Kita-19, Kita-ku, Sapporo 060-0819 Japan.

Keywords: Hydroxyapatite; Carbonate, Albumin, Lysozyme, Adsorption site

Abstract: Carbonate-containing hydroxyapatites (HAp's) were prepared at 6.0, 7.0, 8.5, or 10.5 of pH, and the content of carbonate increased as the increase of pH: 0.9 – 6.3 mass%-CO<sub>3</sub>/g-HAp. Increase of the content made the crystallite size of (001) face smaller by 40 %. IR spectra showed that the increase of carbonate content led to an increase of OH-substituted carbonate species compared to PO<sub>4</sub>-substituted one. The adsorption properties of two kinds of proteins: *acidic* bovine serum albumin (BSA) and *basic* egg white lysozyme (LSZ) were investigated at 295 K on the HAp's of different contents of carbonate. All the adsorption isotherms followed the Langmuir-type adsorption. The saturated-adsorbed amount of BSA decreased with the increase of the content of carbonate. Two reasons were proposed for the decrease of the amount. Firstly, retard of HAp crystal growth along the *c*-axis gave rise to relatively less amount of the *C-site* on *a*- and *b*-faces: less amount of adsorption site for BSA. Secondly, increase of the OH-substituted carbonate may cause less amount of OH vacancy and to inhibit the carboxyl ion of BSA on the *C-site*. LSZ, which is considered to be adsorbed on the *P site* on *c*-face, had little dependency of the content, suggesting that neither crystallographic change nor composition of two kinds of carbonate species had an effect on LSZ adsorption.

(Received March 6, 2007; Accepted April 3, 2007)

### INTRODUCTION

The primary inorganic component in hard tissues such as bones and teeth: Hydroxyapatite {Ca<sub>10</sub>(PO<sub>4</sub>)<sub>6</sub>(OH)<sub>2</sub>: HAp} has been synthesized and used as a ceramic biomaterial. Biological HAp contains carbonate ions (CO<sub>3</sub><sup>2-</sup>) of 3-7 mass %<sup>1</sup>. The carbonate ion causes a decrease in crystallinity of HAp<sup>2</sup>, which is considered to be related to biocompatibility. The roles of the carbonate ion in terms of clinical potentialities in orthopaedics and dentistry were suggested by Cuisinier *et al.*<sup>3</sup>: (1) crystallographic disorder and defect, which favors biological apatite nucleation; (2) increase in solubility, which leads to more calcium and phosphate ions available for further calcification and biological mineralization; and (3) and leads to form stronger metal-biological apatite bonds. However, change in the surface properties of carbonate-containing HAp, in especial, from the viewpoint of adsorption has been unknown. Proteins are intriguing adsorbates because they play variously important roles in a lot of biological function and phenomena. Furthermore, adsorption of proteins on solid materials has been one of hot and challenging topics due to application to drug delivery system<sup>4</sup>.

The surface of HAp has the *C site* on its *a*- and *b*-faces and the *P site* on *c*-face, and the former is considered to be a selective adsorption site for carboxyl and phosphate ions, and the latter for amino

groups<sup>5</sup>. Proteins have the *C*-terminal (-COOH) and the *N*-terminal (-NH<sub>2</sub>), which have different chemical natures, and therefore, examining adsorption properties of proteins on carbonate-containing HAp can give us important information for modification effect of carbonate ion on the surface of HAp.

Two kinds of proteins were employed: an *acidic* protein, bovine serum albumin (BSA) and a *basic* one, egg white lysozyme (LSZ). The dependency of the carbonate content on the adsorbed amounts of these proteins was compared, focusing on modification effects of the carbonate ion on their selective adsorption sites on the surface of HAp.

### MATERIALS AND METHODS

#### (1) Preparation procedure of samples

HAp samples were synthesized in a similar manner to one by Okazaki's<sup>6</sup> in order to control pH rigidly during preparation of HAp samples. Aqueous solution: 0.06 M (NH<sub>4</sub>)<sub>2</sub>HPO<sub>4</sub> was supplied into 0.1 M Ca(NO<sub>3</sub>)<sub>2</sub>·4H<sub>2</sub>O at 4.5 ± 0.5 mL/min with a peristaltic pump. Synthesis of HAp crystal was made under agitation by a magnetic stirrer at 323 ± 5 K, followed by aging for 24 hrs at constant pH with a pH controller (EYELA FC-2000). Introduction of carbonate ion was done by adding NH<sub>4</sub>HCO<sub>3</sub> into (NH<sub>4</sub>)<sub>2</sub>HPO<sub>4</sub>, where molar ratio of Ca: PO<sub>4</sub>: CO<sub>3</sub> was 10 : 6 : 6 at various pH's of 6.0, 7.0, 8.5, or 10.5 under flowing with N<sub>2</sub> gas in the solution. We will

designate the sample with  $\text{NH}_4\text{HCO}_3$  at pH 6.0 as  $C(6)pH6.0$  and one without  $\text{NH}_4\text{HCO}_3$ , which was prepared only at pH 10.5, will be designated as  $C(0)pH10.5$ . The rest of the samples will be designated in this manner of notation.

## (2) Analysis condition

Chemical compounds in the samples were identified by XRD (X-ray diffraction technique, Rigaku RINT 1200). The line source was  $\text{CuK}\alpha$  ( $\lambda = 0.154$  nm), and voltage and current of the tube were 40 kV and 30 mA, respectively. Scanning rate was 4 degrees/min. BET specific surface area was measured by adsorbed amount of nitrogen at 77 K with Shimadzu ASAP 2010. The amount of carbonate was evaluated by TPD (temperature programmed desorption) technique: 0.3 g of sample was loaded in a quartz glass tube of 3 mm i.d. and heated to 1473 K at a rate of 3 K/min in the flow of helium of 30 mL/min (NTP). Under heating the sample, the desorbed amount of  $\text{CO}_2$  gas was measured, which was caused by decomposition of carbonate in HAp structure or other  $\text{CO}_2$ -containing compounds. Analysis of  $\text{CO}_2$  gas was done every three minutes with a gas chromatograph (Shimadzu GC-3BT) attached to a thermal conductivity detector. The obtained  $\text{CO}_2$  spectrum was integrated as a function of time and the amount of carbonate was estimated. Diffuse reflectance infrared fourier transform (DRIFT) spectra were measured at room temperature in air and with Jasco FT-IR 230 to examine location of carbonate in HAp. The detector was MCT, and resolution was  $4\text{ cm}^{-1}$ .

The adsorbed amounts of bovine serum albumin and egg white lysozyme (Sigma-Aldrich Co.) at 295 K were measured for the HAp's with various contents of carbonate. The procedure was as follows: 0.5-3 mg-protein/mL - 20 mM  $\text{K}_2\text{HPO}_4$ - $\text{KH}_2\text{PO}_4$  buffer solutions (pH =  $7 \pm 0.1$ ) of 10 mL were prepared. 0.1 g apatite powder was put in the solution under agitating for 72 hrs. The top clear layer was taken out and centrifuged at 15000 rpm for 30 min and subsequently 18000 rpm for 30 min. The concentration of the protein in the solution was estimated by measuring absorbance at 280 nm with Hitachi UV 2000. The adsorbed amount onto the HAp surface was determined by the difference between the original concentration of the proteins and the conc. in the solution.

## RESULTS AND DISCUSSION

Characterization of HAp samples under various preparing conditions.

### (1) Crystallographic and physical features of the samples under various preparing conditions.

XRD patterns of the samples under various preparing conditions were shown in FIGURE 1. All

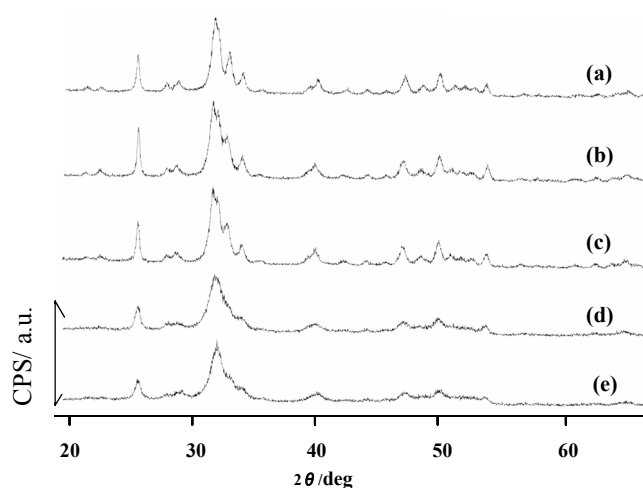


FIGURE 1 XRD patterns of HAp samples under various preparing conditions.

(a)  $C(0)pH10.5$ ; (b)  $C(6)pH6.0$ ; (c)  $C(6)pH7.0$ ; (d)  $C(6)pH8.5$ ; (e)  $C(6)pH10.5$

TABLE 1 Crystallite size of (002) face:  $D(002)$ .

| Sample       | $D(002)^*/\text{nm}$ |
|--------------|----------------------|
| $C(0)pH10.5$ | 30.0                 |
| $C(6)pH6.0$  | 30.8                 |
| $C(6)pH7.0$  | 28.5                 |
| $C(6)pH8.5$  | 19.1                 |
| $C(6)pH10.5$ | 18.1                 |

\* estimated from the XRD peak at  $2\theta = 25.6$  degrees

Table 2. BET specific surface area.

| Sample       | Surface area/ $\text{m}^2\text{ g}^{-1}$ |
|--------------|--|
| $C(0)pH10.5$ | 58.2                                     |
| $C(6)pH6.0$  | 78.2                                     |
| $C(6)pH7.0$  | 125.4                                    |
| $C(6)pH8.5$  | 171.3                                    |
| $C(6)pH10.5$ | 183.6                                    |

the peaks were assigned to those of HAp for all the samples, confirming that HAp was predominantly formed. One can see that the XRD peaks of  $C(6)pH6.0$  are the sharpest and those of  $C(6)pH10.5$  were the broadest among the four  $C(6)$  samples, and degree of growth of HAp crystal is, therefore, sensitive to pH. Crystallite sizes of (002) face of the samples, which are the indices of growth of the crystal along the  $c$ -axis, are compared in Table 1 with Scherrer's equation<sup>7)</sup> by the peak width at half-maximum at  $2\theta = 25.6$  degrees in FIGURE 1. The crystallite sizes were in the order of  $C(6)pH6.0 \cong C(0)pH10.5 > C(6)pH7.0 > C(6)pH8.5 > C(6)pH10.5$ . Generally, increase of pH promotes the crystal growth of HAp because of increase of OH concentration in solution. Therefore, discrepancy between this tendency and the order in TABLE 1 suggests that another factor other than pH is

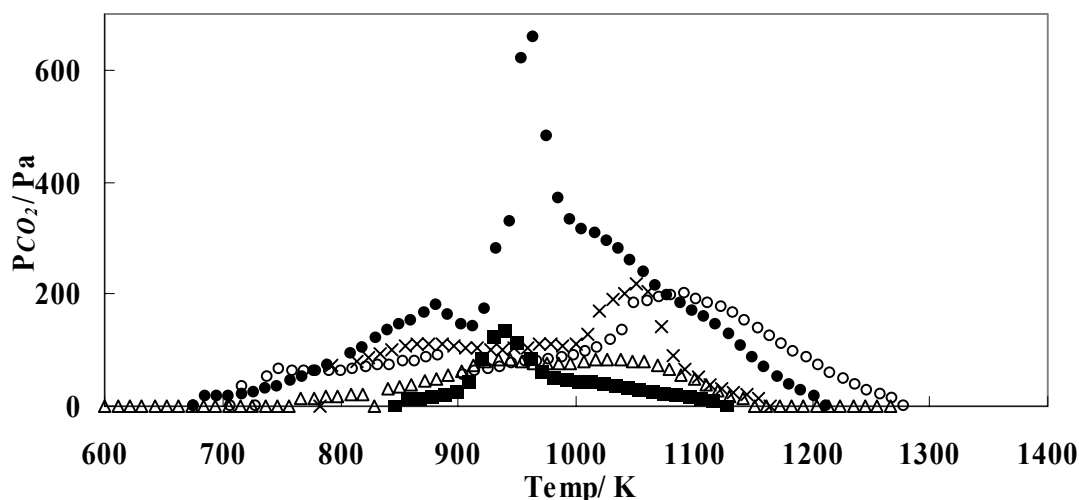


FIGURE 2 TPD spectra of CO<sub>2</sub> for the HAp samples.

○C(0)pH10.5; ■C(6)pH6.0; △C(6)pH7.0; ×C(6)pH8.5; ●C(6)pH10.5

predominant for the crystallographic growth, which will be suggested in terms of the content of the carbonate in the next section.

TABLE 2 shows BET specific surface areas of the samples, and they are in the reverse order of table 1; C(6)pH10.5 > C(6)pH8.5 > C(6)pH7.0 > C(6)pH6.0 > C(0)pH10.5. Both the orders of the crystallite sizes in table 1 and of the surface areas show that retard of crystallographic growth leads to rumpling the surface.

## (2) Characterization of carbonate in HAp.

Temperature programmed desorption (TPD) spectra of CO<sub>2</sub> are shown in FIGURE 2. All the spectra appeared at 700 - 1200 K, which were ascribed to decomposition of carbonates in HAp structure as in our previous paper<sup>8)</sup>. These spectra can be roughly divided into three temperature regions; around 890, 960, and 1060 - 1090 K, indicating existence of three carbonate species with different thermal stability, although resolution of the three spectra were not clear enough to consider correlation of these compositions with the preparing conditions. In order to evaluate the carbonate content in HAp, these spectra are integrated as a function of time with the same manner as in a literature<sup>9)</sup> and the total desorbed amounts of CO<sub>2</sub> were estimated. The results were shown as mass% - CO<sub>3</sub>/g-HAp in FIGURE 3. The content increased as increase of pH for four C(6) samples; 0.92 - 6.3 mass%. The content of C(0)pH10.5 was between those of C(6)pH10.5 and C(6)pH8.5, showing that the content is controlled by pH more than by the presence or absence of NH<sub>4</sub>HCO<sub>3</sub>.

In order to examine difference of the carbonate in more detail, DRIFT spectra of the samples are compared in FIGURE 4(a) and (b), where (a) and (b) are a wavenumber region of carbonate at 1400 - 1550

cm<sup>-1</sup> and that of structural OH at 3568 cm<sup>-1</sup>, respectively. For C(6)pH6.0 (ε), four peaks ascribed to carbonate species in HAp structure were distinguishably observed at 1419, 1456, 1497, and 1540 cm<sup>-1</sup> in (a). A broad peak around 1640 cm<sup>-1</sup> is ascribed to H-OH deformation of adsorbed water.

Nadal *et al.*<sup>10)</sup> suggested that IR spectra of two kinds of carbonate ascribed to in-plane bending vibration: the A-site (OH-substituted) carbonate at 1465 and 1534 cm<sup>-1</sup>, and the B-site (PO<sub>4</sub>-substituted) one at 1430 and 1455 cm<sup>-1</sup> appeared, respectively. Suetsugu *et al.*<sup>11)</sup> prepared a carbonate-apatite single crystal and observed the IR spectra of the two kinds of carbonates at 1410 (the B-site), 1540 (the A-site), and 1460 cm<sup>-1</sup> (complex of the two carbonates). From these reports, the spectra of 1497 and 1540 cm<sup>-1</sup> were assigned to the A-site, and 1419 and 1456 cm<sup>-1</sup> to the B-site carbonates, respectively.

One can see that the relative intensity of the peaks of the A-site carbonate to those of the B-site one got higher gradually from the bottom {C(6)pH6.0; spectrum (ε)} to the top {C(6)pH10.5; spectrum (α)} for four C(6) samples other than C(0)pH10.5, while

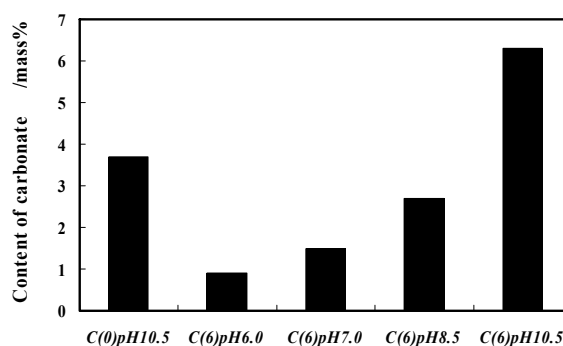


FIGURE 3 The carbonate contents of the HAp samples.

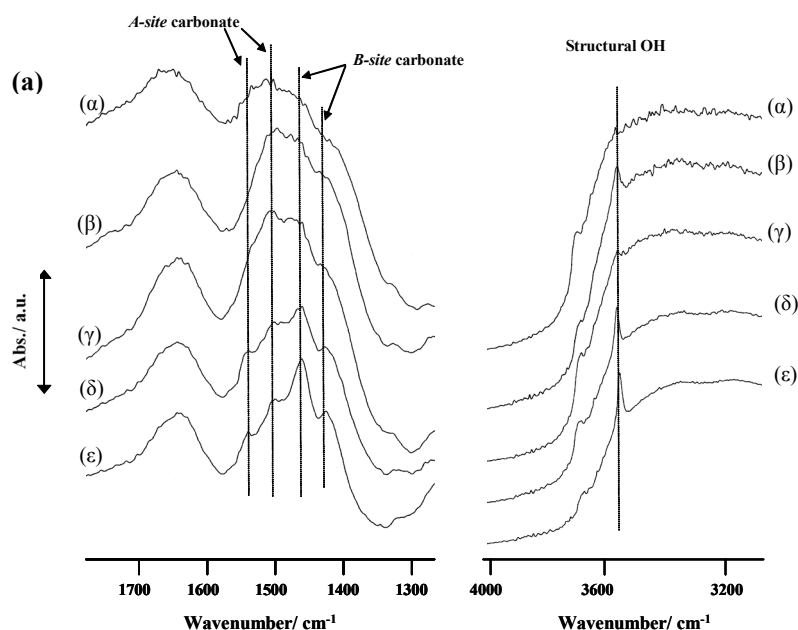


FIGURE 4 DRIFT spectra of the HAp samples of different contents of carbonate. (α)  $C(6)pH10.5$ ; (β)  $C(0)pH10.5$ ; (γ)  $C(6)pH8.5$ ; (δ)  $C(6)pH7.0$ ; (ε)  $C(6)pH6.0$

the intensity of structural OH (b) got lower. The carbonate content was in the order of  $C(6)pH10.5 > C(6)pH8.5 > C(6)pH7.0 > C(6)pH6.0$  for  $C(6)$  samples as shown by Fig. 3. Therefore, increase of the carbonate content led to increase of the amount of the *A-site* carbonate species. This suggests that the carbonate ion is incorporated into HAp structure by substitution for  $PO_4$  primarily and then for OH. In  $C(0)pH10.5$  {spectrum (β)}, the peak intensity of the *A-site* carbonate was lower than those of  $C(6)pH8.5$  {spectrum (γ)} and that of the structural OH of spectrum (β) was higher than that of spectrum (γ), although the carbonate content of  $C(0)pH10.5$  was larger than that of  $C(6)pH8.5$ . This may suggest that incorporation mechanism of the carbonate ion for  $C(0)$  is different from  $C(6)$  samples.

Adsorption behavior of BSA and LSZ on the HAp samples of various carbonate contents.

The adsorption properties of bovine serum albumin (BSA) and egg white lysozyme (LSZ) on the five HAp samples of various carbonate contents were measured. FIGURE 5(a) and (b) show adsorption isotherms of BSA and LSZ at 295 K, where the vertical axes are the adsorbed amounts:  $V$  as a function of concentration of BSA or LSZ in the solution:  $C_e$ . All the isotherms tended to plateau with increase of the concentration of BSA or LSZ. Langmuir plots obtained from FIGURE 5(a) or (b) are shown in FIGURE 6(a) or (b), where the vertical axes are  $C_e/V$  vs.  $C_e$ . They gave straight lines indicating the Langmuir-type adsorption<sup>12</sup>; single-layer adsorption under our experimental condition as shown by the previous paper<sup>13</sup>. The

slope of each line gave reciprocal saturated-adsorbed amount, and the amounts thus estimated are plotted as a function of the contents of the carbonate in FIGURE 7. The results were shown as mg-BSA or mg-LSZ/m<sup>2</sup>-HAp for offsetting the difference of surface areas, which are closely connected with adsorption, of the samples. The amount of BSA decreased with an increase of the content of the

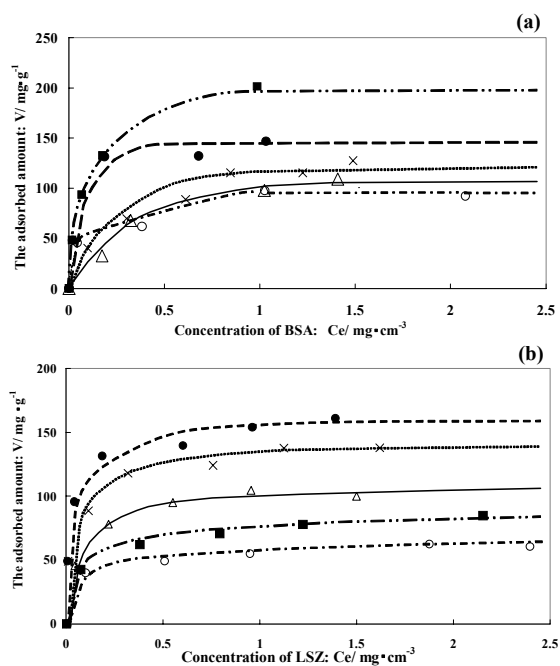


FIGURE 5 Adsorption isotherms of (a)BSA and (b)LSZ at 295 K. ○ $C(0)pH10.5$ ; ■ $C(6)pH6.0$ ; △ $C(6)pH7.0$ ; × $C(6)pH8.5$ ; ● $C(6)pH10.5$

carbonate while that of LSZ did not show so much differences. However, the amounts of  $C(0)pH10.5$  were seen to deviate from these relations, which may reflect a different mechanism of incorporation of the carbonate as mentioned in the last section.

The difference of the dependency of the carbonate content on the adsorbed amounts of BSA and LSZ was discussed from the viewpoint of the modification effect of the carbonate on surface adsorption sites. It has been suggested that BSA adsorbs selectively on the  $C$ -site of  $a$ - (or  $b$ -) face of HAp crystal, and this site is the position of OH with neighboring two Ca on the edge of  $a$ - (or  $b$ -) face<sup>14</sup>. Furthermore, the existence of the OH vacancy on the surface of HAp was suggested by Zahn and Hocherein<sup>15</sup> with a molecular dynamics simulation. They suggested that the Schottky OH vacancy in the sublattice of HAp crystal favored migration across the calcium triangles forming a (001) channel to the surface. BSA is an *acidic* protein with 4.7 - 4.9 of isoelectric point, and therefore the  $C$  terminal exists as carboxyl anion in our experimental condition; pH 7. It should be a possibly stable adsorption form of BSA that the carboxyl anion locating the OH vacancy interacts with Ca ion of HAp. DRIFT spectra in Fig. 4 showed that increase of the carbonate led to increase of the OH-substituted carbonate, possibly indicating decrease of the amount of surface OH vacancies because DRIFT spectra gives information mainly on the surface. Therefore, the decrease of the amount of adsorbed BSA in FIGURE 7 may have caused by the increase of the  $A$ -site (OH-substituted) carbonate.

Furthermore, the other possible cause is difference of crystallographic properties depending on the carbonate content. As the carbonate content increased, crystal growth along  $c$ -axis was retarded for  $C(6)$  samples as shown in TABLE 1. This means the decrease of relatively exposed area of  $a$ - and  $b$ - faces, leading to the decrease of the area available for BSA adsorption.

In contrast to BSA, the adsorbed amount of LSZ was not dependent on the carbonate content. LSZ is suggested to be adsorbed mainly on the  $P$  site of the  $c$ -face, the position of Ca (possibly Ca vacancy) surrounded by six oxygen atoms of three phosphate ions<sup>5</sup>. As LSZ is a *basic* protein with 11.0 -11.4 of isoelectric point, amino cation of LSZ locating the Ca vacancy can interact with phosphate anion, based on similar consideration in the case of BSA. In our samples, phosphate ions were partly substituted by the carbonate ion. Existence of the  $B$ -site ( $PO_4$ -substituted) carbonate on the surface did not seem to change character of the  $P$  site of the  $c$ -face so much as the  $A$ -site (OH-substituted) carbonate on the  $C$  site of  $a$ - and  $b$ -faces because of the Ca vacancy of the  $P$ -site being kept. On the other hand, a question remains from the viewpoint of the crystallographic change, for the adsorbed amount of LSZ did not differ in spite of the relative increase of the exposed

area of  $c$ -face to  $a$  ( $b$ )-face as the increase of the carbonate content. More information on the difference of microscopically crystallographic features of the samples may be necessary to clarify this question.

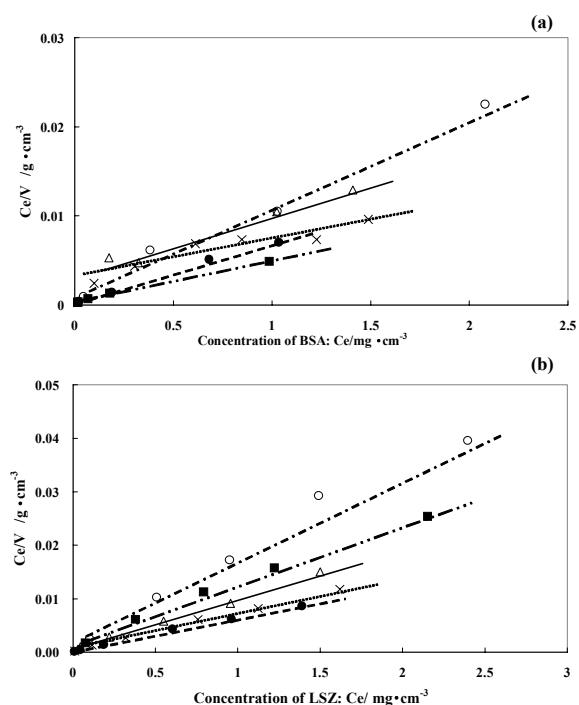


FIGURE 6 Langmuir plots of (a)BSA and (b)LSZ at 295 K.  $\circ$  $C(0)pH10.5$ ;  $\blacksquare$  $C(6)pH6.0$ ;  $\triangle$  $C(6)pH7.0$ ;  $\times$  $C(6)pH8.5$ ;  $\bullet$  $C(6)pH10.5$

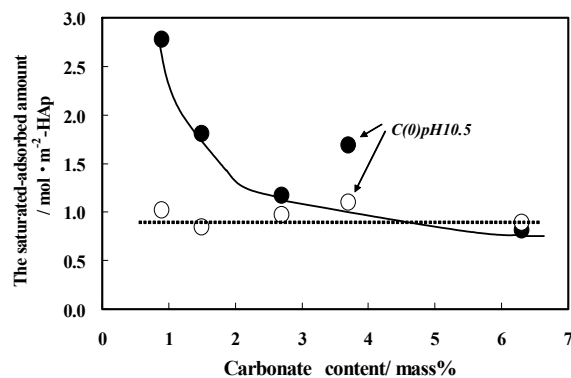


FIGURE 7 The adsorbed amounts of BSA( $\bullet$ ) and LSZ( $\circ$ ) vs. the carbonate content.

## CONCLUSIONS

The dependency of the carbonate content in HAp on adsorption of proteins was different depending on their *acid-base* character in a neutral condition. The adsorbed amount of an *acidic* protein, bovine serum albumin decreased with increase of the carbonate content, which was ascribed to occupation of the OH

vacancy on the HAp surface and retardation of crystallographic growth along the *c*-axis by the carbonate. This result may suggest that the carbonate in biological hard tissues under neutral condition has a similar effect on adsorption of *acidic* proteins or other biological substances. Investigating desorption behavior of proteins from the carbonate-modified HAp is intriguing and necessary for both basic and practical views, and is underway also in our group.

#### REFERENCES

1. H. Aoki, *Apatite* (Ishiyaku-shuppan Inc, Tokyo, 1999), pp. 19.
2. M. Okazaki, Y. Moriwaki, T. Aoba, Y. Doi, J. Takahashi, *Caries Res.* **15**, 477 (1981).
3. F-J-G. Cuisinier, P. Steuer, J-C. Voegel, F. Apfelbaum, I. Mayer, *J. Mater. Sci.: Mater. in Medicine*, **6**, 85 (1995).
4. D-J. Maxwell, B-C. Hicks, S. Parsons, S-E. Sakiyama-Elbert, *Acta Biomaterialia*, **1**(1), 101 (2005).
5. T. Kawasaki, *J Chromatography*, **157**(3), 7 (1978).
6. M. Okazaki, J. Takahashi, *Biomaterials*, **20**, 1073 (1999).
7. G. Matumura, *X-senn Kaisetu Yo-ron*, (Agune Inc, Tokyo, 1980), pp. 93-94.
8. T. Kanno, J. Horiuchi, M. Kobayashi, Y. Motogami, T. Akazawa, *J Ceram Soc Jpn*, **107**(6), 517 (1999).
9. T. Kanno, M. Kobayashi, *Nippon Kagakukai-shi*, No. 10, 774 (1995).
10. M. Nadal, J-C. Trombe, G. Bonel, G. Montel, *J. Chim. Phys.*, **67**, 1161 (1970).
11. Y. Suetsugu, I. Shimoya, J. Tanaka, *J. Am. Ceram. Soc.*, **81**(3), 746 (1998).
12. I. Langmuir, *J. Am. Chem. Soc.*, **40**(9), 1361 (1918).
13. T. Akazawa, M. Kobayashi, *J. Ceram. Soc. Jpn.*, **104**(4), 284 (1996).
14. T. Kawasaki, *J. Chromatography*, 151, 95 (1978).
15. D. Zahn, O. Hochrein, *Z. Anorg. Allg. Chem.*, **631**, 1134 (2005).